RESEARCH ARTICLE

Macromolecular Chemistry and Physics
www.mcp-journal.de

Magnetic Properties of a Polyfluorene Derivative Metallopolymer Containing Neodymium Ions

*Alisson J. Santana, Denis A. Turchetti, Cristiano Zanlorenzi, José C. R. dos Santos, Adilson. J. A. de Oliveira, and Leni Akcelrud**

The magnetic properties of a polyfluorene derivative, {Poly[9,9'-dihexylfluorene-2,7-yl)-3,8-(1,10-phenanthroline)]} and its complexes with neodymium ions are explored and discussed in the light of the macromolecular configuration and photophysical properties. The pristine noncomplexed material is a diamagnetic material, and the introduction of Nd atoms in the polymer leads to a paramagnetic behavior over the entire temperature range. The prominent role of the morphology is demonstrated by comparison of two forms, with different ligands to the metal: one with bulky β-diketone groups and another with small chorine as ligands. The large groups hinder interchain interaction, whereas the smaller salt forms favored interchain π-stacking, providing a better interaction of the magnetic field with the polymer backbone, resulting in enhanced magnetic properties. The form with the β-diketone groups exhibits a paramagnetic behavior whereas the one in the salt form presents ferromagnetic behavior at room temperature. This contribution brings solid confirmation to the importance of interchain interaction in the magnetic properties of conjugated polymers, opening a new way to the obtainment of magnetic conjugated polymers.

1. Introduction

The discovery of conducting conjugated polymers, in the last decades of the past century, breaking the belief that plastics were inherently dielectrics, was a milestone in materials science. From the seminal work of Heeger, McDiarmid, Shirakawa[1] together with the Cambridge group[2] a new avenue for photovoltaics,[3–7] LEDs,[8–12] sensors,[13–15] and field effect transistors,[16–19] opened wide. The next step following was the development of polymers with magnetic properties. Magnetic field effects on organic semiconductors were demonstrated already in the early nineties.[20,21] However, molecule-based magnets as opposite to classical inorganic ones began to show solid results in the present century. The intriguing features in these systems and their potentiality in technological applications arose huge interest in scientific and industrial communities.[22]

Conducting polymers are particularly interesting in this regard because their conjugation length is much higher than in small molecules and oligomers, and this is an important feature together with other specific molecular characteristics for the development of magnetic properties. Significant effort has been devoted to the obtainment of processable polymer materials possessing magnetic behavior, mainly by ion doping using polyaniline,[23–25] P3HT,[26–29] and electrochemical synthesis. Purely organic π conjugated systems without doping or metallic insertion presenting magnetic properties at low temperatures include highly crosslinked macrocyclic structures[30] and covalently linked triazine-based radical frameworks, in which the neighboring radicals interact ferromagnetically.[31] Other contributions include copolymer structures based on Schiff´s bases and the heteroaromatic bithiazole, having small walled nanotubes in one end. The bithiazole double bonds were the loci for the coordination for Nd^{3+},[32] C_{60} and Fe^{2+}.[33]

More recent approaches consider that apart from the chemical structure of the polymer, the macromolecular architecture plays a key role in the magnetic behavior of the bulk material, notably chain ordering and planarity. Studies with P3HT,[26] PANI,[34] and the works of Peters introducing substituents of various degrees of bulkiness into poly(3-alkylthiophene)s[35] exemplify this assumption. Mataga et al[36] have demonstrated that electron-spin exchange interactions can occur quite strongly through the π conjugation system, as compared to interactions through space in molecular solids. This approach carries an important potential for the obtainment of magnetic properties at ambient temperature,[37] as demonstrated in the results shown here. In a recent publication,[38] we have demonstrated that a conjugated chain, namely Poly[9,9'-dihexylfluorene-2,7-diyl)-6,6"-(2,2':6':2"-terpyridine)], (an alternated copolymer of fluorene and terpyridine) complexed with neodymium was able to amplify fourfold the magnetization response of the corresponding low molecular weight material. Thus, these behaviors indicate that the mobile π electrons play

A. J. Santana, D. A. Turchetti, C. Zanlorenzi, L. Akcelrud
Paulo Scarpa Polymer Laboratory (LaPPS) Federal University of Parana
POB 19081, Curitiba, Parana 81531-990, Brazil
E-mail: leni@ufpr.br
J. C. R. dos Santos, A. J. A. de Oliveira
Physics Department
Federal University of Sao Carlos
POB 676, São Carlos, SP 13565-905, Brazil

The ORCID identification number(s) for the author(s) of this article can be found under https://doi.org/10.1002/macp.202100289

DOI: 10.1002/macp.202100289

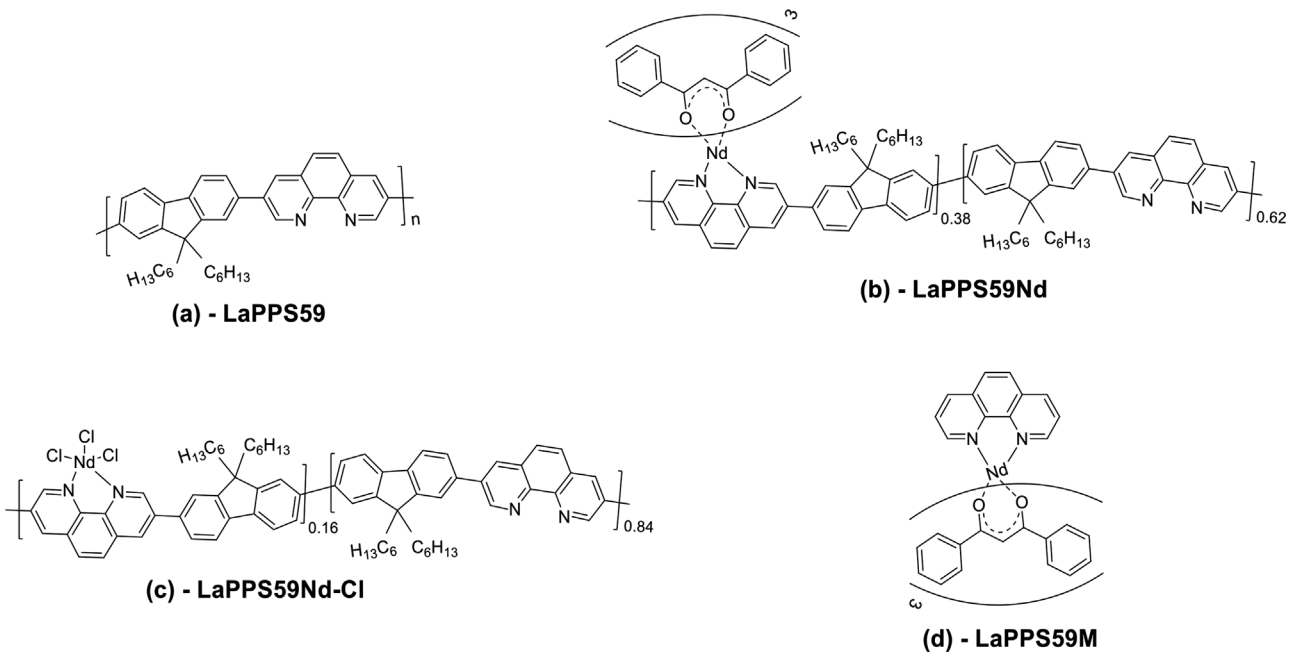

Figure 1. Chemical structures of the a) pristine polymer (LaPPS59), of the b) metallopolymer with dibenzoylmethane as a ligand (LaPPS59Nd), of the c) metallopolymer ion (LaPPS59Nd-Cl) and of the model compound simulating the complexed site (LaPPS59M). The ligand in LaPPS59Nd and in the model compound (LaPPS59M) is dibenzoylmethane (DBM).

an important role for the obtainment of magnetic properties in organic solids, which was accounted for the interaction of the mobile electrons of the rare earth metal and the conducting band of the polymer. Moreover, it was demonstrated that the intermolecular π stacking of the polymer brought about macroscopic effects enhancing furthermore this interaction.[38,39] Considering the consensus that the π-stacking between the chains enhances the electronic interaction polymer-metal,[38,39] we designed a molecule similar to the previous one by changing the terpyridine moiety by 1,10-phenanthroline. This would impart rigidity and planarity, thus increasing intermolecular association not found in the terpyridine copolymer, because the pyridine rings in this case are able to assume several conformations, thus somehow hampering the intermolecular association. Attempting to correlate the magnetic properties with structural and morphological features, the following compounds were explored: the alternated copolymer of fluorene and phenanthroline in its noncomplexed form, Poly[9,9'-dihexylfluoren-2,7-yl)-3,8-(1,10-phenanthroline)] (LaPPS59), one complexed form containing the metal with dibenzoylmethane (DBM) ligands (LaPPS59Nd), and another complexed one in salt form (LaPPS59Nd-Cl).

Phenanthroline has a rigid geometry with three coplanar aromatic rings, two nitrogen atoms and excellent chelating capacity,[40] affording good properties to materials aiming optoelectronic and magnetic applications. The rationale supporting the project proved to be a solid one: the materials showed magnetic properties at 300 K.

The chemical structure of the pristine polymer (LaPPS59) and of the complexed forms (LaPPS59Nd) and (LaPPS59Nd-Cl) are shown in **Figure 1**a–c, respectively. A model compound (LaPPS59M) was also synthesized to simulate coordinated sites. The acronym LaPPS is derived from the Laboratory's name and the number represents the order of its preparation. In this case, the polymer is the 59th structure synthesized. The polymer was produced by a simple, well known chemical route (Suzuki polycondensation), using common chemical compounds (fluorene and phenanthroline) as starting materials, is soluble in usual organic solvents as THF and chloroform.

Significant work was out using metallopolymers,[35] combining a conjugated backbone with a metallic part, mostly using lanthanides.[41]

In this Figure Nd is represented as pentacoordinated, for simplicity. Nd was purchased in the salt form ($NdCl_3$).$6H_2O$, then the three Cl atoms in LaPPS59Nd-Cl. When inserted in the polymer, two of the water molecules were replaced by the phenanthroline ligand, but four of them remain bound to the lanthanide, which is then 9-coordinated.

2. Results and Discussion

2.1. Structural Characterization

The polymer (LaPPS59) was prepared through the cross-coupling Suzuki polycondensation and the metallopolymers (LaPPS59Nd / LaPPS59Nd-Cl) were synthesized following reported procedures.[38] A model compound (LaPPS59M) was synthesized to simulate complexed sites as shown in Scheme 1 in Supporting Information.

The weight average molecular weight of the noncomplexed form was Mw = 7400 g mol^{-1} with polydispersity 1.72 measured by GPC. The chemical structure was confirmed by ^1H and ^{13}C NMR (Figure S1 and S2 in Supporting Information) and FTIR spectra (Figure S3 in Supporting Information).

Thermal Gravimetric Analysis (TGA) showed that the degradation temperatures ($Td_{5\%}$) (Figure S4 in Supporting Information) were 220 °C (LaPPS59), 320 °C (LaPPS59M), 250 °C (LaPPS59Nd) and 240 °C (LaPPS59Nd-Cl). The complex content, determined by TGA (oxide residue) gave a value of 16% and 38% (molar basis) for LaPPS59Nd-Cl and LaPPS59Nd, respectively. DSC curves for LaPPS59, LaPPS59Nd-Cl and LaPPS59Nd (Figure S5 in Supporting Information) showed the onset of glass transition about 121 °C, 126 °C and 128 °C, respectively. The increase in the glass transition indicates that the ion insertion stiffened the polymer chain.

In the FTIR (Figure S3 in Supporting Information) of the pristine polymer (LaPPS59) strong bands were observed in two regions, 700–900 and 1200–1650 cm^{-1}. The ones at 729 and 823 cm^{-1} were assigned to the out of plane vibrations of the C–H bonds in the heterocyclic rings and to the C–H bonds in the phenanthroline ring,[43–45] respectively. The band at 729 cm^{-1} shifted to low frequency for the LaPPS59Nd-Cl appearing at 723 cm^{-1} due to coordination. The band at 823 cm^{-1} was not affected by complexation. This was expected since the primary effect of coordination is on the nitrogen atom, and the central ring has no nitrogen atom to provide any donor site.[43–45] More intense bands and characteristics of the LaPPS59 vibrational spectrum appear in the 1200–1650 cm^{-1} region, referring to stretching modes ν(C=C) and ν(C=N). All these bands on the LaPPS59Nd-Cl have shifted to higher frequencies. The frequency of vibrations in the plane increases with coordination, while those outside the plane decrease. The largest change in frequency is found in the vibrations involving the stretch modes ν(C=C) and ν(C=N). This was anticipated since coordination takes place on nitrogen and the effect is transmitted throughout the region resulting in the readjustment of the electron density.[43–45]

In the LaPPS59Nd and LaPPS59M spectra, three characteristic bands were prominent, ranging from 1408 to 1595 cm^{-1}, attributed to the stretching vibrations ν(C=C), ν(C=N) and ν(C=O), the latter assigned to the DBM ligand. The ν(C=C) related to aromatic rings practically did not change for both. In a general way, it was observed that coordination increased the absorption frequency of conjugated sites.

2.1. Photophysical Properties

The absorption and emission spectra of the three polymers in THF solution are depicted in **Figure 2**, and the absorption spectrum of the model compound in Figure S6 in Supporting Information. The absorption of the pristine polymer (LaPPS59, noncomplexed) presented a broad band, without vibronic structure centered at 370 nm. The complexed form (LaPPS59Nd, with DBM ligands) also had a broad band centered at 370 nm, with a vibronic contribution seen at 353 nm. This could be accounted to a better inter chain separation, due to the bulkiness of the DBM ligands, as previously observed in similar metallopolymer systems.[46] LaPPS59Nd-Cl presented a broad band at 376 nm encompassing the absorption of the other samples. In the absorption spectra of Figure 2, it was not possible to detect the transitions of the Nd ion, due to the higher absorption of the organic part in relation to the metallic one. These were observed only at higher concentrations, as shown in Figure S7 in Supporting Information.

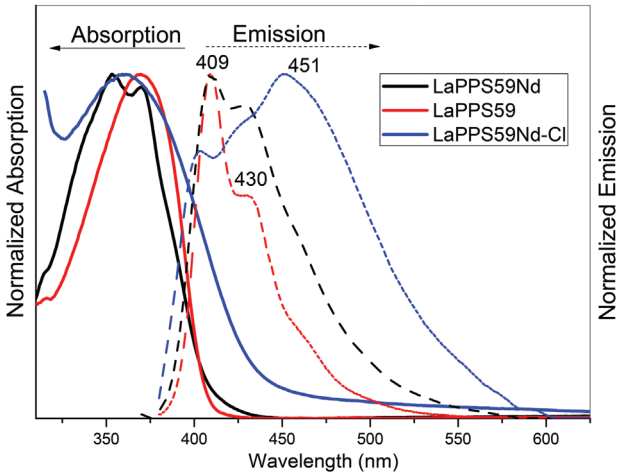

Figure 2. Absorption and emission (λ_{ex} = 370 nm) normalized spectra of LaPPS59 (red line), LaPPS59Nd (black line), and LaPPS59Nd-Cl (blue line) in THF 10^{-5} mol L^{-1} solution.

Analyzing the emission, it can be observed that for LaPPS59 and for LaPPS59Nd the spectra present bands peaking at 409 and 430 nm. The latter can be accounted to a vibronic band usually seen in fluorene based conjugated polymers.[47] A dramatic change in profile of LaPPS59Nd-Cl was noted. The bands at 409 and 430 nm are still present, but attenuated, a somewhat larger spectral overlap (absorption versus emission) could be contributing to this effect. But the most striking feature is the high emission at 451 nm strongly red shifted in relation those of the other polymers.[46,48–50] This spectral behavior is typical of aggregated structures that could be formed as a result of the absence of the bulky DBM substituents (as compared to LaPPS59Nd) and to the possibility of the Nd ion to complex with another phenanthroline unit from a neighboring chain. This would approximate the chains increasing the degree of the π-stacking, consequently red shifting the emission spectrum. The effect was also found in the case of a Schiff base-bithiazole copolymer complexed with Nd^{3+}[51] and of PANI nanocomposites through bridges of MnO_4.[52]

The spectra in the solid state are shown in **Figure 3**. The deaggregating effect brought about by the bulky $(DBM)_3$ was manifested, an emission at 450 nm was seen for LaPPS59Nd (black line) whereas for the other samples the emission was 15–20 nm redshifted (red and blue lines).

Considering that the three copolymers differ only in the nature of the complexed sites (backbone without complexation, coordinated sites with $Nd(DBM)_3$ and with $NdCl_3$), it seemed valuable to compare the differences in geometry of the three forms. **Figure 4** illustrates the optimized geometries of the corresponding tetramers and related radii. It was verified that the LaPPS59Nd polymer has a large backbone radius (11.9 angstroms), brought about by the extra volume added by $Nd(DBM)_3$, whereas in the LaPPS59Nd-Cl the $NdCl_3$ substituent did not contribute significantly to the polymer radius. In other words, the pristine backbone and the complexed one with $NdCl_3$ have approximately the same radii (8.5 angstroms), and the

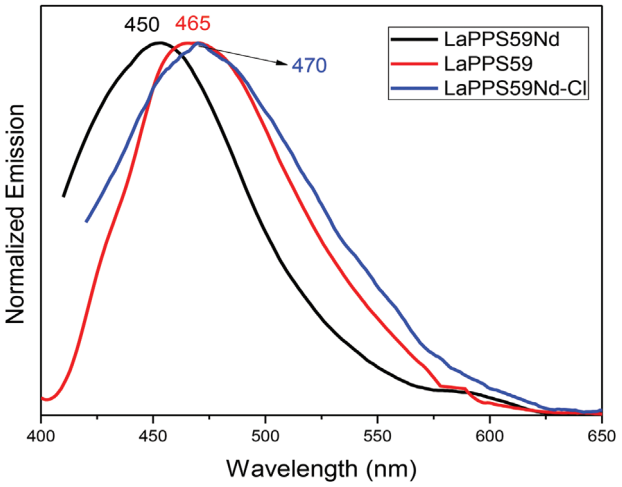

Figure 3. Emission spectra in solid state of LaPPS59 (red line), LaPPS59Nd (black line), e LaPPS59Nd-Cl (blue line). $\lambda_{ex} = 370$ nm.

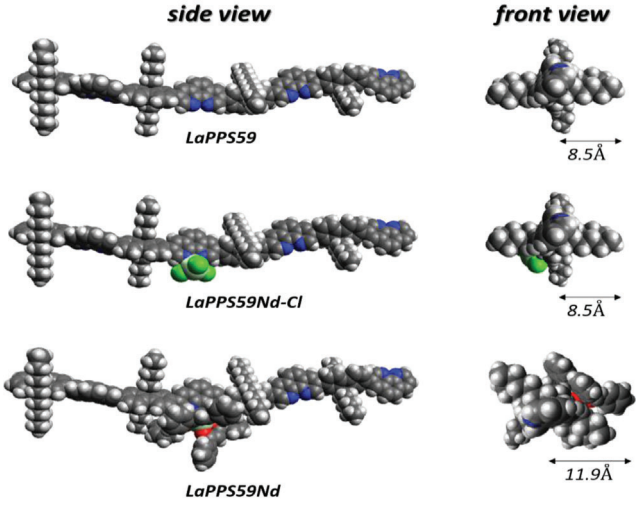

Figure 4. Space filling models of optimized ground state geometries of three polymers LaPPS59Nd-Cl, LaPPS59Nd, and LaPPS59.

DBM substituted form is 1.4 times larger. These morphological differences would result in better planarity and proximity in the systems without the large steric hindrance brought about by the bulky DBM ligands, which in turn will affect profoundly the magnetic properties. The coincidence of the bathochromic shifts observed in Figure 3 for the pristine polymer and for the one complexed in the salt form agree with these theoretical results.

2.2. Magnetic Properties

Figure 5a,b displays the DC magnetic susceptibility $\chi_{DC} = \frac{M}{H}$ as a function of temperature, performed using the ZFC protocol with an applied magnetic field of $H = 100$ Oe and magnetization as a function applied magnetic at 300 K for pristine backbone. Both measurements confirmed diamagnetic behavior observed in all range of temperature, due to the response to magnetic field of the backbone electrons. Figure 5a exhibited a small dependence with temperature associated to the promotion of core electrons due to temperature effects. However, this contribution is very small and represents approximately 10% in all range of temperature.

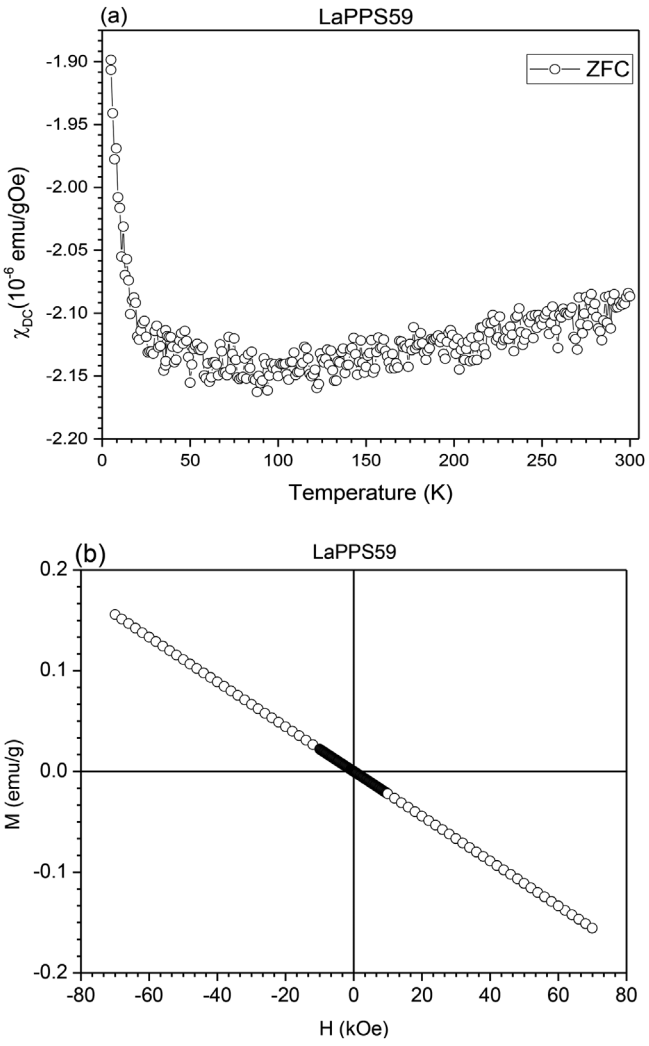

Figure 5. DC magnetic susceptibility ($\chi_{DC} = \frac{M}{H}$) as a function of temperature, performed using the ZFC protocol with an applied magnetic field of $H = 100$ Oe a) and magnetization as a function of the applied field at 300 K in powder sample of LaPPS59 b).

Figure 6 presents magnetic characterization of samples LaPPS59Nd and LaPPS59M. In all results the diamagnetic contribution was subtracted from linear fitting in high field. In (a) and (b) are shown the magnetization measurements as a function of applied magnetic field at 300 K for LaPP59Nd and LaPPS59M, respectively. The linear behavior presented in both samples is a characteristic of paramagnetic material at room temperature. This magnetic behavior is corroborated by the magnetic susceptibility measurements $\chi_{DC} = \frac{M}{H}$ as a function of the temperature, using ZFC and FC protocols with an applied field of $H = 100$ Oe. Magnetic irreversibility is not observed in these measurements, which is an indication of the absence of strong magnetic interaction between magnetic moments. This

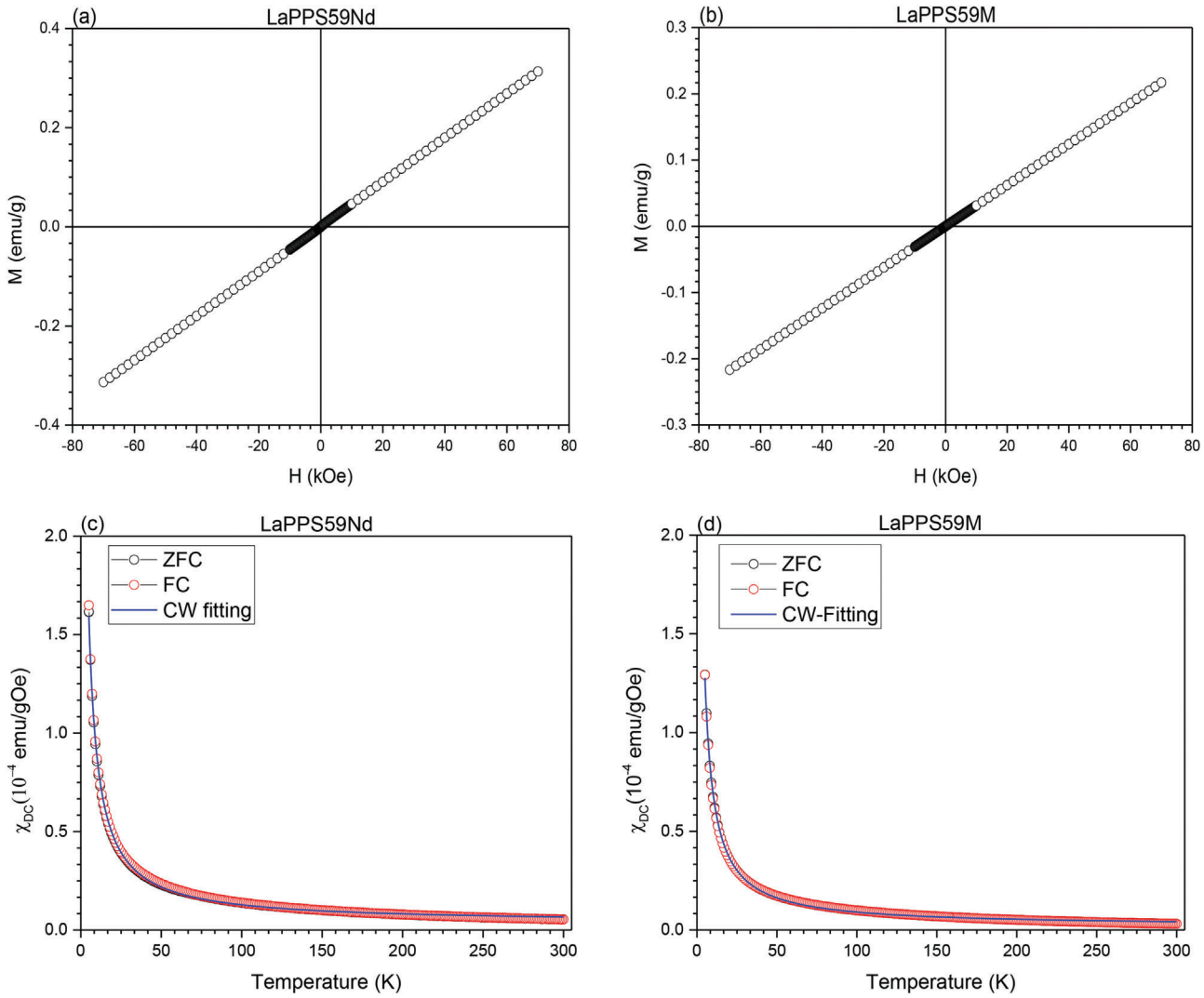

Figure 6. Magnetic characterization of samples LaPPS59Nd and LaPPS59M. a,b) Magnetization as a function of applied magnetic field at 300 K. c,d) DC magnetic susceptibility as a function of the temperature, using zero-field-cooled (ZFC) (black line) and field-cooled (FC) (red line) protocols were used, with an applied field of 100 Oe. Blue line is the Curie-Weiss fitting, performed in FC curve.

Table 1. Fitting parameters for samples LaPPS59Nd, LaPPS59M and LaPPS59Nd-Cl from Equation (1).

Sample	$C(\frac{\text{emu K}}{\text{g Oe}})$	θ [K]
LaPPS59Nd	1.171×10^{-3}	–2.72
LaPPS59M	0.849×10^{-3}	–1.99

behavior is better understood from the fitting, performed in FC curves, using Equation (1)

$$\chi_{DC} = \frac{C}{T - \theta} \quad (1)$$

where C is a Curie constant, θ is Curie-Weiss temperature. Fitting parameters are shown in **Table 1**.

Magnetic characterizations show that the introduction of Nd atoms in both structures led to a paramagnetic behavior, where the value of $\theta < 0$ is an indication that mean field of interaction magnetic moments induced an antiferromagnetic alignment. Measurements using ZFC and FC protocols do not exhibit thermomagnetic irreversibilities, corroborating this hypothesis. Another important point is that both samples present similar values of Curie constant. Commonly, in mean filed theory the value of C is associated to exchange interaction between local magnetic moments. However, concerning to lanthanide-based complexes one needs to consider not only exchange interactions, but also crystal fields effects, where this effect is more relevant due to the crystal field splitting the ground J multiplet.[53] However, sample LaPPS59Nd-Cl exhibited a more complex behavior. One major point that needs to be considered here is that in lanthanide molecular crystals the ion is in a fixed position, subjected to forces that govern the exchange interactions. When the ion is inserted into a conjugated polymer chain, it suffers the influence of high mobile π surrounding electrons. The subject has been addressed recently in the literature,[38] but a definitive

explanation of the nature of interactions polymer-ion has yet to be found. The experimental results showed that magnetic properties can be very much altered, not only by the presence of the polymer backbone itself but also by the inter-macromolecular interaction forces. In other words, inter-macromolecular π-stacking is favorable to enhance the magnetic outcome. Moreover, the more rigid the polymer chain, more prone to the stacking the system is, due to the enhancement of the electronic delocalization. In another contribution,[38] we have used a similar polymer to the one explored in this work, with the difference that here we have used phenanthroline in place of the t-pyridine used previously. The rationale for that is that phenanthroline is a condensed three ring system much more rigid than the t-pyridine, that allows a degree of rotation between its three rings. Therefore, phenanthroline would facilitate the π-stacking.

Figure 7 shows the results relative to magnetization as a function applied. magnetic field (MxH) at 300 K (a) and magnetic susceptibility as a function of temperature performed at $H = 100$ Oe using ZFC/FC protocol. In both measurements, the diamagnetic contribution was subtracted. In (a) we observed a characteristic ferromagnetic behavior at 300 K, with saturation magnetization (Ms), remanent magnetization and coercive field (Hc) in the same order observed in other materials based on carbon ferromagnets at room temperature, as conducting polymers[28,54–56] and graphene systems.[57] These values are presented in **Table 2**.

Figure 7b shows magnetic susceptibility as a function of temperature performed with ZFC/FC protocol. The fitting calculated in FC measurement was performed with a CW law modified as Equation (2)

$$\chi_{DC} = \frac{C}{T-\theta} + \chi_0 \tag{2}$$

where χ_0 is a constant parameter proportional to the ferromagnetic contribution. All magnetic parameter of Figure 7 are presented in Table 2.

The magnetic characterizations of samples show that the pristine backbone sample exhibits diamagnetic contribution only. The introduction of Nd atoms in LaPPS59Nd and LaPPS59M samples led to a paramagnetic behavior, over the entire temperature range. Fitting parameters of the two samples show a Curie-Weiss contribution, where the Curie constant has approximately the same values for both samples. The small value of the Weiss temperature (around –1K) is an indication that the interaction between magnetic moments is antiferromagnetic. On the other hand, sample LaPPS59Nd-Cl presents a weak ferromagnetic behavior at room temperature. The introduction of Nd^{3+} ion led to the weak ferromagnetic interaction due to small magnetization saturation (15 memu g^{-1}) as compared to the magnetization value of paramagnetic samples at 70 kOe (0.3 emu g^{-1}). The magnetic susceptibility shows a Curie-Weiss behavior; but the Curie constant is around 10 times smaller,indicating that a minor part of magnetic moments is interacting paramagnetically. In addition, the Weiss temperature for this sample is very small, but is positive, characteristic of ferromagnetic interaction between magnetic moments. Finally, χ_0 parameter introduced in the fitting is associated a ferromagnetic contribution, which in this case it is practically independent of the temperature, indicating

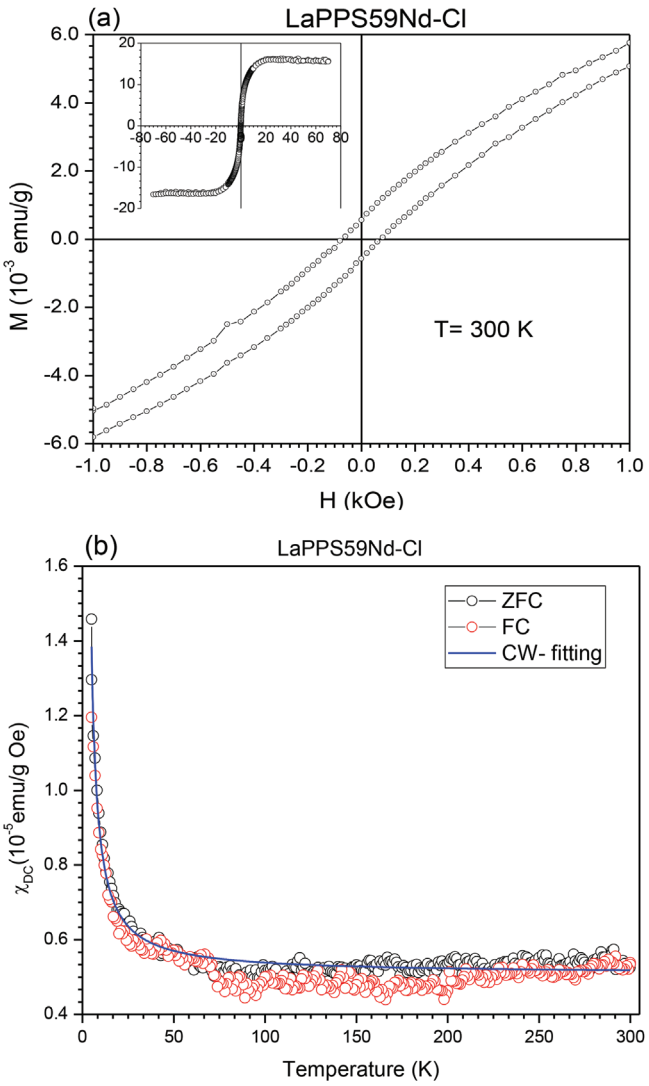

Figure 7. a) Magnetization as a function of the applied field at 300 K with details of hysteresis loop. The inset shows complete measurements. b) Magnetic susceptibility as a function of the temperature, using the procedure zero-field-cooled (ZFC) (black line) and field-cooled (FC) (red line) with an applied field of 100 Oe for LaPPS59Nd-Cl in powder form.

that the ferromagnetic interaction must persist for temperatures above room temperature, in a small part of the sample. These results strengthen the findings related in the previous paper.[38] It may also be added that the observed magnetic behavior for the LaPPS59Nd-Cl sample shows a relatively small saturation magnetization, in the order of 15×10^{-3} emu/g, indicating a weak ferromagnetism. However, as magnetic moment measurements are normalized by the total mass of the sample, only a part of the

Table 2. Magnetic parameters and CW fitting parameters for samples LaPPS59Nd-Cl from Equation (2).

Polymer	$M_S(\frac{emu}{g})$	$M_R(\frac{emu}{g})$	$H_C(Oe)$	$C(\frac{emu \cdot K}{g \cdot Oe})$	$\theta(K)$	$\chi_0(\frac{emu \cdot K}{g \cdot Oe})$
LaPPS59Nd-Cl	15×10^{-3}	6×10^{-4}	80	2.995×10^{-5}	1.58	5.08×10^{-6}

polymer can contribute to the observed magnetic moment. The fitting performed using Equation (2) shows that the sample has a paramagnetic contribution (Curie-Weiss) added to a constant that represents the ferromagnetic contribution, as noted in ref.[38] There is a possibility that there is an antiferromagnetic interaction between the Nd ions, as indicated for the LaPPSNd sample because $\theta(K) < 0$. However, for sample LaPPS59Nd-Cl we found $\theta(K) > 0$ indicating ferromagnetic coupling. We also observed that the value of the Curie constant being much smaller than that observed in the other samples, is an indication that the paramagnetic portion of the sample contributes little to the total magnetization, at 300 K. Thus, the Nd ions in the sample LaPPS59Nd-Cl are weakly coupled.

3. Conclusions

The comparison between the complexed with the noncomplexed conjugated polymers showed that the insertion of the Nd^{3+} imparted a ferromagnetic behavior to the pristine noncomplexed material. The main factor for associated to this result is the strengthening of the assumption that secondary and tertiary structures are crucial for achieving the desired cooperative magnetic properties.[22] The pristine, noncomplexed polymer (LaPPS59) is a diamagnetic material. When $Nd(DBM)_3$ is inserted via complexation into the phenanthroline moiety (LaPPS59Nd) a paramagnetic behavior is observed. The complexation also brings about a decrease in the intermolecular interaction due to the bulkiness of the DBM ligand. A calculated value for the radius of the molecule increases from 8.5 angstroms without the DBM ligand (pristine and complexed in the salt form) to 11.9 angstroms with the ligand. The shifting observed in the solid-state emission spectra of the materials further corroborates this result. The pristine form showed a peak at 470 nm, whereas in the complexed one it appears at 450 nm. It is accepted in the literature[38,39,58,59] that π-stacking favors the interaction of the magnetic field with the polymer backbone, thus improving the magnetic properties. The behavior of the complexed form with Nd^{3+} ions having Cl^- as counter ions reflects the outcome of this steric condition: the planarity and rigidity of the phenanthroline unit, together with the little disturbance in chain diameter with the inclusion of $NdCl_3$. On top of that the possibility of the linking of the Nd cation of one chain to another, bringing them close together further improving the π-stacking, resulted in the magnetic outcome described.

It is noteworthy that to be applied as a useful magnetic material some requirements must be fulfilled. These include the maintenance of the magnetic properties at operating temperatures (RT mainly), which is present in the LaPPS59Nd-Cl sample.

4. Experimental Section

Materials: Potassium carbonate (Vetec, 99%), 3,8-dibromo-1,10-phenanthroline (TCI America), tetrakis (triphenylphosphine) palladium (0) (Aldrich, 99%), 9,9'-dihexylfluorene-2,7-diboronic-acid-bis(1,3-propanediol)ester (Aldrich, 97%), Neodymium (lll) chloride hexahydrate (Aldrich, 99.9%). Dichloromethane (Synth, 99.5%), tetrahydrofuran (Synth, 99.8%), toluene (Aldrich, 99.3%), methanol (Aldrich, 99. 6%). Deuterated chloroform, containing 1% (v/v) TMS (Sigma-Aldrich, P.A.) as standard for the NMR analyses, was used. For purification a medium pressure chromatographic column, with silica as a stationary phase, from Merck, 230 mesh, was used.

Measurements: ^1H and ^{13}C NMR spectra were recorded on a Varian Inova-400 Instrument at 400 MHz with polymer solution containing deuterated chloroform ($CDCl_3$) and TMS as reference. The FTIR spectra were performed on KBr pellets using the BOMEM (Hartmann & Braun) MB-Series equipment scanning rate of 4000–400 cm^{-1} and 24 scans min^{-1} The polymer molecular weight was determined by Gel Permeation Chromatography (GPC), using polystyrene as standards and THF HPLC as eluent. Thermogravimetric analyses (TGA) were carried out under nitrogen at a heating rate of 20 °C min^{-1} with Netzsch Thermisch Analyzer TG 209 analyzer. Differential scanning calorimetric (DSC) were measured on a Netzsch DSC 204 F1. All samples were heated from 20 to 200 °C in a nitrogen atmosphere and then cooled to 20 at 10 °C min^{-1}, with scanning rate of the 10 °C min^{-1} and nitrogen flow 15 mL min^{-1}. UV–Vis spectra was measured on a Shimadzu UV-3101PC spectrometer in THF solution. The emission studies were measured on a Shimadzu RF–5301PC in THF solution and solid state. Magnetic measurements were performed using a Quantum-Design Magnetometer (MPMPS3) with SQUID-VSM (vibrating sample magnetometry combine SQUID sensor) technique. Magnetization as a function of temperature (MxT) were performed using de zero-field cooling (ZFC) and field cooling (FC) protocols at 2 K min^{-1} and magnetization measurements as a function applied magnetic field (MxH) were taken up to 300 K.

Chemical Procedures: The chemical pathways for the synthesis described low are illustrated in Scheme 1 on the Supporting Information.

Polymer Synthesis of Poly[9,9'-Dihexylfluorene-2,7-yl)-3,8-(1,10-Phenanthroline)] (LaPPS59): 9,9'-dihexylfluorene-2,7-diboronic-acid-bis(1,3-propanediol)ester (0.300 g, 0.597 mmol), 3,8-dibromo-1,10-phenanthroline (0.201 g, 0.597 mmol) and potassium carbonate (2.21 g, 15.59 mmol) were added to a round bottomed flask with high neck under an argon atmosphere. After 3 cycles of argon and vacuum, 12 mL of toluene and 4 mL of distilled water were added under stirring. Tetrakis(triphenylphosphine)-palladium(0) (0.024 g, 0.021 mmol) was dissolved in toluene (2 mL) and added dropwise to the solution. After stirring for 72 h at 110 °C, the polymer was re-precipitated with methanol. Impurities and oligomers were eliminated by Soxhlet extraction using methanol. The polymer was filtered and dried under vacuum for 48 h, resulting in 0.190 g of product. ^{13}C NMR ($CDCl_3$, 200 MHz): δ (ppm) 152.47, 151.32, 149.96, 149.64, 144.83, 144.73, 144.38, 140.94, 137.59, 136.71, 136.38, 133.62, 133.46, 129.72, 128.78, 128.19, 127.31, 126.81, 126.45, 125.97, 121.98, 120.91, 119.83, 119.23, 55.78, 40.38, 31.49, 29.66, 23.97, 22.57, 14.02. FT-IR(KBr): 2923 (m), 2852 (s), 1604 (m), 1463 (w), 1419 (s), 1369 (w), 1309 (m), 1245 (m), 1112 (m), 1095 (m), 1002 (w), 895 (m), 823 (s), 729 (s).

Metallopolymer Synthesis with DBM Ligands (LaPPS59Nd): Polymer LaPPS59 (0.080 g, 0.156 mmol), dibenzoylmethane (DBM) (0.466 g, 0.468 mmol) and triethylamine (0.260 mL) were dissolved in dried THF (20 mL) under argon. Neodymium (III) chloride hexahydrate (0.056 g, 0.156 mmol) was dissolved in methanol (3 mL) and added dropwise to the solution. After stirring for 24 h at 60 °C, the solvent was removed under reduced pressure. The yellow solid was filtered in a Buchner funnel and washed with methanol. FT-IR(KBr): 2925 (m), 2854 (m), 1595 (s), 1548 (s), 1517 (s), 1477 (m), 1456 (m), 1407 (s), 1307 (w), 1220 (w), 1070 (w), 1024 (w), 721 (m), 688 (w), 607 (w).

Metallopolymer Synthesis without DBM Ligands (LaPPS59Nd-Cl): Polymer LaPPS59 (0.080 g, 0.156 mmol), was dissolved in dried THF (20 mL) under argon. Neodymium(III) chloride hexahydrate (0.056 g, 0.156 mmol) was dissolved in methanol (3 mL) and added dropwise to the solution. After stirring for 24 h at 60 °C, the solvent was removed under reduced pressure. The brown solid was filtered in a Buchner funnel and washed with methanol. FT-IR(KBr): 2923 (s), 2852 (s), 1622 (s), 1465 (s), 1423 (w), 1375 (m), 1311 (m), 1249 (w), 1105 (m), 1095 (m), 905 (w), 823 (s), 723 (s).

Model Compound Synthesis (LaPPS59M): LaPPS59M was synthesized following the procedure described.[38] Briefly, 1,10-phenanthroline (0.080 g, 0.444 mmol), dibenzoylmethane (0.299 g, 1.332 mmol) and 0.2 mL of triethylamine were dissolved in dry THF (20 mL) under ar-

gon. Neodymium (III) chloride hexahydrate (0.159 g, 0.444 mmol) was dissolved in methanol (3 mL) and added dropwise to the solution. After stirring for 24 h at 60 °C, the solvent was removed under reduced pressure. The white solid was filtered on a Buchner funnel and washed with methanol and n-hexane. FT-IR(KBr): 3056 (m), 3024 (w), 2925 (w), 1593 (s), 1548 (s), 1517 (s), 1477 (s), 1456 (s), 1409 (s), 1309 (m), 1220 (m), 1176 (w), 1068 (m), 1024 (m), 939 (w), 840 (m), 723 (s), 690 (m), 607 (m).

Theoretical Calculations: The optimized ground state geometry of the three polymers LaPPS59Nd-Cl, LaPPS59Nd and LaPPS59 was calculated at the RM1 level, and using SPARKLE model to Lanthanide Complexed polymers, both as implemented in MOPAC 2016.[42] From these tetramer geometries, the diameters of the polymer chains were theoretically estimated.

Supporting Information

Supporting Information is available from the Wiley Online Library or from the author.

Acknowledgements

This study was financed in part by the Coordenação de Aperfeiçoamento de Pessoal de Nível Superior – Brasil (CAPES) – Finance Code 001. The authors wish to acknowledge to UFPR (Federal University of Parana), CNPq (National Council for Scientific and Technological Development), INEO (National Institute for Organic Electronics) and FAPESP (2013/07296-2 and 09/54082-2).

Conflict of Interest

The authors declare no conflict of interest.

Data Availability Statement

The data that support the findings of this study are available from the corresponding author upon reasonable request.

Keywords

ferromagnetism, magnetic polymers, metallopolymers

Received: August 3, 2021
Revised: November 26, 2021
Published online: December 19, 2021

[1] H. Shirakawa, *Curr. Appl. Phys.* **2001**, *1*, 281.
[2] J. H. Burroughes, D. D. C. Bradley, A. R. Brown, R. N. Marks, K. Mackay, R. H. Friend, P. L. Burns, A. B. Holmes, *Nature* **1990**, *347*, 539.
[3] M. Kim, W.-T. Park, S. U. Ryu, S. Y. Son, J. Lee, T. J. Shin, Y.-Y. Noh, T. Park, *Chem. Mater.* **2019**, *31*, 4864.
[4] S.-I. Na, S.-H. Oh, S.-S. Kim, D.-Y. Kim, *Org. Electron.* **2009**, *10*, 496.
[5] C. Zanlorenzi, L. Akcelrud, *J. Polym. Sci., Part B: Polym. Phys.* **2017**, *55*, 919.
[6] L. Li, R. G. Hadt, S. Yao, W.-Y. Lo, Z. Cai, Q. Wu, B. Pandit, L. X. Chen, L. Yu, *Chem. Mater.* **2016**, *28*, 5394.
[7] H. Zhou, L. Yang, W. You, *Macromolecules* **2012**, *45*, 607.
[8] M. Marumoto, T. Sotani, Y. Miyagi, T. Yajima, N. Sano, F. Sanda, *Macromolecules* **2020**, *53*, 2031.
[9] B. Nowacki, H. Oh, C. Zanlorenzi, H. Jee, A. Baev, P. N. Prasad, L. Akcelrud, *Macromolecules* **2013**, *46*, 7158.
[10] L. Akcelrud, in *Physical Properties of Polymers Handbook* (Ed: J. E. Mark), 2nd ed., Springer, Cincinnati, OH **2007**, pp. 757–782.
[11] J. C. Germino, J. N. De Freitas, R. A. Domingues, F. J. Quites, M. M. Faleiros, T. D. Z. Atvars, *Synth. Met.* **2018**, *241*, 7.
[12] C. Chakraborty, A. Layek, P. P. Ray, S. Malik, *Eur. Polym. J.* **2014**, *52*, 181.
[13] D. Abbaszadeh, A. Kunz, N. B. Kotadiya, A. Mondal, D. Andrienko, J. J. Michels, G.-J. A. H. Wetzelaer, P. W. M. Blom, *Chem. Mater.* **2019**, *31*, 6380.
[14] D. Jaque, F. Vetrone, *Nanoscale* **2012**, *4*, 4301.
[15] V. Vohra, T. Anzai, *J. Nanomater.* **2017**, *2017*, 1.
[16] K. Hwang, M.-H. Lee, J. Kim, Y.-J. Kim, Y. Kim, H. Hwang, I.-B. Kim, D.-Y. Kim, *Macromolecules* **2020**, *53*, 1977.
[17] L. Zhang, Z. Wang, C. Duan, Z. Wang, Y. Deng, J. Xu, F. Huang, Y. Cao, *Chem. Mater.* **2018**, *30*, 8343.
[18] H. Kajii, Y. Ie, M. Nitani, Y. Hirose, Y. Aso, Y. Ohmori, *Org. Electron.: Phys., Mater., Appl.* **2010**, *11*, 1886.
[19] H. Kajii, K. Koiwai, Y. Hirose, Y. Ohmori, *Org. Electron.: Phys., Mater., Appl.* **2010**, *11*, 509.
[20] E. L. Frankevich, A. A. Lymarev, I. Sokolik, F. E. Karasz, S. Blumstengel, R. H. Baughman, H. H. Hörhold, *Phys. Rev. B* **1992**, *46*, 9320.
[21] H. Zhao, R. A. Heintz, X. Ouyang, K. R. Dunbar, C. F. Campana, R. D. Rogers, *Chem. Mater.* **1999**, *11*, 736.
[22] J. S. Miller, A. J. Epstein, *MRS Bull.* **2000**, *25*, 21.
[23] V. T. Santana, O. R. Nascimento, D. Djurado, J. P. Travers, A. Pron, L. Walmsley, *J. Phys.: Condens. Matter* **2013**, *25*, 116004.
[24] D. Djurado, A. Pron, J.-P. Travers, J. G. S. Duque, P. G. Pagliuso, C. Rettori, D. L. Chingalia, L. Walmsley, *J. Phys.: Condens. Matter* **2008**, *20*, 285228.
[25] D. Djurado, A. Pron, J. F. Jacquot, J. P. Travers, C. Adriano, J. M. Vargas, P. G. Pagliuso, C. Rettori, G. G. Lesseux, I. Fier, L. Walmsley, *J. Phys.: Condens. Matter* **2011**, *23*, 206004.
[26] S. Majumdar, J.-O. Lill, J. Rajander, H. Majumdar, *Org. Electron.: Phys., Mater., Appl.* **2015**, *21*, 66.
[27] N. A. Zaidi, S. R. Giblin, I. Terry, A. P. Monkman, *Polymer* **2004**, *45*, 5683.
[28] F. R. de Paula, E. C. Pereira, A. J. A. de Oliveira, *J. Supercond. Novel Magn.* **2010**, *23*, 127.
[29] F. R. De Paula, L. Walmsley, E. C. Pereira, A. J. A. De Oliveira, *J. Magn. Magn. Mater.* **2008**, *320*, 193.
[30] A. Rajca, J. Wongsriratanakul, S. Rajca, *Science* **2001**, *294*, 1503.
[31] J. Mahmood, J. Baek, *Chem* **2019**, *5*, 1012.
[32] B. He, W. Sun, M. Wang, Z. Shen, *Mater. Chem. Phys.* **2004**, *87*, 222.
[33] L. Jiang, W. Sun, J. Weng, Z. Shen, *Polymer* **2001**, *43*, 1563.
[34] N. A. Zaidi, S. R. Giblin, I. Terry, A. P. Monkman, *Polymer* **2004**, *45*, 5683.
[35] L. M. C. Pereira, L. Dillemans, H. Peeters, M. Jivanescu, G. Koeckelberghs, J. Locquet, M. J. Van Bael, *Polym. Chem.* **2014**, *52*, 76.
[36] N. Mataga, *Theor. Chim. Acta* **1968**, *10*, 372.
[37] A. Rajca, J. Wongsriratanakul, S. Rajca, *Science* **2001**, *294*, 1503.
[38] A. J. Santana, D. A. Turchetti, C. Zanlorenzi, J. C. R. Santos, E. Laureto, A. J. A. De Oliveira, L. Akcelrud, *J. Polym. Sci., Part B: Polym. Phys.* **2019**, *57*, 304.
[39] G. Pan, F. Chen, L. Hu, K. Zhang, J. Dai, F. Zhang, *Adv. Funct. Mater.* **2015**, *25*, 5126.
[40] T. Wang, H. Wang, G. Li, M. Li, Z. Bo, Y. Chen, *Macromolecules* **2016**, *49*, 4088.
[41] M. Cardoso Dos Santos, A. Runser, H. Bartenlian, A. M. Nonat, L. J. Charbonnière, A. S. Klymchenko, N. Hildebrandt, A. Reisch, *Chem. Mater.* **2019**, *31*, 4034.

[42] J. Stewart, *MOPAC2016; Stewart Computational Chemistry (SCC)* **2016**.
[43] J. Zhang, L.-X. Wang, L. Zhang, Y. Chen, Q.-T. Zhang, *Rare Met.* **2016**, *32*, 599.
[44] S. S. Singh, *Zeitschrift für Naturforschung* **1968**, *25*, 2015.
[45] M. M. Campos-Vallette, R. E. Clavijo, F. Mendizabal, W. Zamudio, R. Baraona, G. Diaz, *Vib. Spectrosc.* **1996**, *12*, 37.
[46] D. A. Turchetti, P. C. Rodrigues, L. S. Berlim, C. Zanlorenzi, G. C. Faria, T. D. Z. Atvars, W. H. Schreiner, L. C. Akcelrud, *Synth. Met.* **2012**, *162*, 35.
[47] P. C. Rodrigues, I. Grova, D. J. Coutinho, R. A. Domingues, H. S. Oh, J. Seo, R. M. Faria, T. D. Z. Atvars, P. N. Prasad, L. Akcelrud, *J. Polym. Res.* **2012**, *19*, 9828.
[48] E. C. G. Campos, C. Zanlorenzi, B. F. Nowacki, G. M. Miranda, D. A. Turchetti, L. C. Akcelrud, *Adv. Condens. Matter Phys.* **2018**, *2018*, 1.
[49] S. M. Cassemiro, C. Zanlorenzi, T. D. Z. Atvars, G. Santos, F. J. Fonseca, L. Akcelrud, *J. Lumin.* **2013**, *134*, 670.
[50] U. Lemmer, S. Heun, R. F. Mahrt, U. Scherf, M. Hopmeier, U. Siegner, E. O. Göbel, K. Müllen, H. Bässler, *Chem. Phys. Lett.* **1995**, *240*, 373.
[51] B. He, W. Sun, M. Wang, Z. Shen, *Mater. Chem. Phys.* **2004**, *87*, 222.
[52] B. H. Shambharkar, S. S. Umare, R. C. Rathod, *Trans. Indian Inst. Met.* **2014**, 67.
[53] D. Parker, E. A. Suturina, I. Kuprov, N. F. Chilton, *Acc. Chem. Res.* **2020**, *53*, 1520.
[54] A. A. Correa, L. Walmsley, L. O. S. Bulhões, W. A. Ortiz, A. J. A. De Oliveira, E. C. Pereira, *Synth. Met.* **2001**, *121*, 1836.
[55] O. R. Nascimento, A. J. A. de Oliveira, A. A. Correa, L. O. S. Bulhões, E. C. Pereira, V. M. Souza, L. Walmsley, *Phys. Rev. B: Condens. Matter Mater. Phys.* **2003**, *67*, 1.
[56] L. M. C. Pereira, L. Dillemans, H. Peeters, M. Jivanescu, G. Koeckelberghs, J. Locquet, M. J. Van Bael, *Polym. Chem.* **2014**, *52*, 76.
[57] X. Jiang, Y. Liu, T. Wang, B. Xia, J. Qian, J. Ran, Z. Zhang, D. Gao, *J. Magn. Magn. Mater.* **2021**, *538*, 168223.
[58] M. González M, H. Osiry, M. Martínez, J. Rodríguez-Hernández, A. A. Lemus-Santana, E. Reguera, *J. Magn. Magn. Mater.* **2019**, *471*, 70.
[59] M. González, A. A. Lemus-Santana, J. Rodríguez-Hernández, M. Knobel, E. Reguera, *J. Solid State Chem.* **2013**, *197*, 317.

